Applied Catalysis B: Environmental 99 (2010) 81–88

Contents lists available at ScienceDirect

Applied Catalysis B: Environmental

journal homepage: www.elsevier.com/locate/apcatb

Behavior of steam reforming reaction for bio-ethanol over Pt/ZrO_2 catalysts

Tatsuya Yamazaki[a,*], Naoko Kikuchi[a], Masahiro Katoh[b], Toyoko Hirose[a], Hiroaki Saito[c], Takushi Yoshikawa[d], Mamoru Wada[d]

[a] Department of Basic Sciences, Faculty of Science & Engineering, Ishinomaki Senshu University, Shin-mito 1, Minamizakai, Ishinomaki, Miyagi 986-8580, Japan
[b] Department of Advanced Materials, Institute of Technology and Science, The University of Tokushima, Minamijosanjima-cho 2-1, Tokushima, Tokushima 770-8506, Japan
[c] Graduate School of Engineering, Tohoku University, 6-6-07 Aramaki-Aoba, Aoba-ku, Sendai 980-8579, Japan
[d] Sanwa Cornstarch Co. Ltd., 594 Unate-cho, Kashihara, Nara 634-8585, Japan

ARTICLE INFO

Article history:
Received 22 May 2009
Received in revised form 3 June 2010
Accepted 3 June 2010
Available online 15 June 2010

Keywords:
Bio-ethanol
Ethanol steam reforming
Platinum catalyst
Hydrogen formation
Deactivation

ABSTRACT

Steam reforming reactions of reagent ethanol and of biomass-derived ethanol (bio-ethanol) over Pt catalysts supported on ZrO_2 were studied. For steam reforming reactions at 673 K of reagent ethanol with an H_2O/C_2H_5OH molar ratio = 3, the initial H_2 yields were 20–29%. The major carbon-containing products were CH_4, CO_2, and CO. Small amounts of acetaldehyde, acetone, and ethylene were produced, showing that the partial ethanol steam reforming reaction ($C_2H_5OH + H_2O \rightarrow CH_4 + CO_2 + 2H_2$) occurred competitively with the ethanol decomposition reaction ($C_2H_5OH \rightarrow CH_4 + CO + H_2$).

H_2 formation for bio-ethanol was less than that obtained with reagent ethanol under the same conditions. The catalytic activity for the partial steam reforming reaction decreased rapidly; a similar decrease in the activity of the ethanol decomposition reaction was observed. The poisoning effect of sulfur compounds on the Pt sites was responsible for the deactivation of the bio-ethanol steam reforming reaction.

1. Introduction

Biomass-derived ethanol (bio-ethanol), produced from energy plants such as corn and sugarcane by saccharification and/or fermentation [1,2], is a renewable energy resource. Recently, the use of bio-ethanol has received considerable attention with a view to harnessing its potential environmental benefits. The conventional use of bio-ethanol is as a motor fuel, usually blended with gasoline. However, the cost and energy involved in meeting the strict standards imposed in many countries on the quality of bio-ethanol used for motor fuel [3,4] have inhibited the use of bio-ethanol.

Steam reforming of ethanol has several advantages: (1) the water present in bio-ethanol can be used as a reactant; (2) the product, H_2, is insoluble in water; and (3) the reaction proceeds at a low temperature, which can be attained using waste heat. In addition, thermodynamic analysis shows that equilibrium H_2 yields as high as 5.5 mol per mol of ethanol in the feed are obtainable when the reaction conditions are optimized [5,6]. Studies of ethanol steam reforming catalysts have therefore increased significantly in recent years [7–14].

Catalyst deactivation is a problem that must be overcome in the steam reforming reaction. The influence of carbon deposition on catalyst deactivation has been studied [10,15–17]. However, there is still uncertainty as to the deactivation mechanism because the reaction mechanism is very complex and deactivation factors other than coking have been little discussed. Elucidation of the deactivation mechanism and identification of the catalytic poisons in bio-ethanol are important issues in steam reforming of bio-ethanol containing impurities other than water. However, few studies use real bio-ethanol as a reactant [17–19]. The properties of bio-ethanol depend strongly on its purity. However, even bio-ethanol of relatively high purity (even the approximately 80% pure bio-ethanol used in this work) has a slightly yellowish-brown color and a peculiar aroma, showing that the effects of minor impurities other than water on the reaction may be unavoidable. In the development of a process using bio-ethanol, it is important to identify the impurities that actually affect the catalytic reaction.

The present study is one of a series of research efforts aimed at verifying the effectiveness of using bio-ethanol in the steam reforming process. The properties of Pt/ZrO_2 as catalysts for the ethanol steam reforming reaction at low temperatures were examined using bio-ethanol by-produced in the fermentation process in cornstarch production. The properties of the bio-ethanol reaction were analyzed by comparing them with those for the reaction using reagent ethanol (the model reactant). We attempted to clarify the

* Corresponding author. Tel.: +81 0225 22 7716; fax: +81 0225 22 7746.
E-mail address: t_ymzk@isenshu-u.ac.jp (T. Yamazaki).

0926-3373/$ – see front matter © 2010 Elsevier B.V. All rights reserved.
doi:10.1016/j.apcatb.2010.06.003

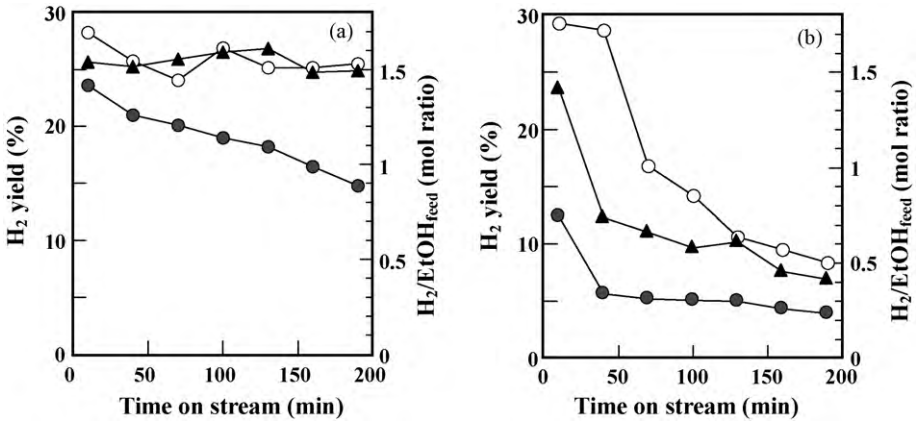

Fig. 1. H_2 yield (%) for ethanol steam reforming reaction at 673 K (a) and at 773 K (b); (●) $Pt/ZrO_2(1)$, (▲) $Pt/ZrO_2(3)$, and (○) $Pt/ZrO_2(5)$. Right ordinate means ratio of H_2 formation rate (mol/min) to EtOH feed rate (mol/min).

deactivation factors for the bio-ethanol reaction and to highlight the problems for bio-ethanol use.

2. Experimental

2.1. Catalyst and reactant materials

It has been reported that Pt shows high activity for biomass gasification [20] and for steam reforming of oxygenated hydrocarbons such as acetic acid [21]. Accordingly, $Pt/ZrO_2(n)$, where n is the Pt loading (wt%), catalysts were prepared by incipient wetness impregnation of zirconia (JRC-ZRO-2) using an aqueous solution of $H_2PtCl_6{\cdot}6H_2O$ (Wako JIS Special grade, Wako Pure Chemicals Industry, Ltd., Osaka, Japan). The catalysts were dried at 383 K overnight and then calcined at 873 K in an air stream for 4 h. The Pt loadings were 1–5 wt%.

Bio-ethanol derived from corn (Sanwa Cornstarch Industry Co., Ltd., Nara, Japan) was used. This bio-ethanol is a slightly brown liquid, comprising mainly water (19.6 wt%) and ethanol (77.4 wt%), with residual amounts of methanol (1.6 wt%), acetaldehyde (1.7 wt%), and n-propanol (0.4 wt%); its pH is 6.07. The reactant was prepared by adding distilled water to the bio-ethanol until the H_2O/C_2H_5OH molar ratio reached a value of 3. An aqueous solution of reagent ethanol (H_2O/C_2H_5OH molar ratio of 3) was used as a reference sample.

2.2. Catalyst characterization

The specific surface areas of the products were evaluated by the BET method at 77 K using N_2 gas as the adsorbate. The amounts of N_2 adsorbed were obtained by a constant-pressure-type adsorption apparatus after the samples had been pretreated by evacuation for 2 h at 623 K. The X-ray powder diffraction (XRD) patterns for the samples were obtained using a Rigaku X-ray diffractometer (Rigaku Corporation, Tokyo, Japan; X-ray source at 40 kV, 20 mA for Cu-Kα radiation; time constant 2 s; and scan speed 5°/min).

The surface composition and surface deposits were analyzed by X-ray photoelectron spectroscopy (XPS), using a Scienta ESCA-200 spectrometer (VG Scienta; X-ray source, Al-Kα at 400 W and 14.7 kV; pressure in the sample chamber, less than 1.0×10^{-4} Pa). The XPS spectrometer was equipped with a flood gun, which was used to compensate for the surface charge build-up.

The amount of Pt active sites was measured by the CO pulse adsorption method using a flow type adsorption cell. 0.1–0.2 g of catalyst was heated to 673 K under a He gas flow, and reduced for 1 h at 673 K under an H_2 gas flow (*ca.* 40 mL/min). After the sample was cooled down room temperature under He gas flow, CO pulse adsorption (pulse size is 23.8 μmol) was carried out in He flow (*ca.* 30 mL/min). CO consumption was evaluated by gas chromatograph equipped with TCD.

2.3. Reaction

The catalyst (0.2 g), molded to a grain size of 1–2 mm, was set in a fixed-bed flow-through reactor, and then reduced at the desired temperature (673 K or 773 K, the same temperatures as used for the catalytic tests) for 1 h under an H_2 flow (50 mL/min) before the reaction. The reactant solution was supplied to the reactor via a plunger-pump-type liquid delivery unit at 0.0925 g/min (WHSV≒12.8 h^{-1} for C_2H_5OH) using an N_2 gas flow (50 mL/min) as the reactant carrier. Catalytic tests were then carried out at 673/773 K at atmospheric pressure. The gaseous products were analyzed by gas chromatography after passing through an ice trap. The liquid samples accumulated in the ice trap were also analyzed by gas chromatography.

3. Results and discussion

3.1. Reaction properties of aqueous ethanol solution

To clarify the fundamental properties of Pt/ZrO_2 catalysts for ethanol steam reforming, catalytic tests on an aqueous ethanol solution ($H_2O/C_2H_5OH = 3$), prepared using reagent ethanol (S grade 99.5%; Wako Pure Chemicals Industry, Ltd., Osaka, Japan), were carried out. Fig. 1a and b shows the H_2 yields (%) as a function of time-on-stream at 673 K and 773 K. In this work, the H_2 yield (%) is defined as the ratio of the amount of H_2 produced to that produced if the ethanol steam reforming reaction ($C_2H_5OH + 3H_2O \rightarrow CO_2 + 6H_2$) went to completion [6]:

$$H_2 \text{ yield } (\%) = \left[\frac{\text{mol of produced } H_2}{\text{mol of EtOH feed} \times 6}\right] \times 100$$

At 673 K (Fig. 1a), the catalysts loaded with 3–5 wt% of Pt ($Pt/ZrO_2(3)$ and $Pt/ZrO_2(5)$) exhibited H_2 yields of over 25%. In addition, the H_2 yields were generally stable with respect to time-on-stream (<3 h), showing that catalyst deactivation did not occur. The H_2 yields corresponded to 1.5 mol per mol of ethanol feed; the largest H_2 space time yield (STY), 8 mmol/min/g_{cat}, was obtained with the $Pt/ZrO_2(5)$ catalyst. The activity of the $Pt/ZrO_2(1)$ catalyst was small even in the initial stages, and the activity decreased gradually. At 773 K, the initial activities of the $Pt/ZrO_2(3)$ and $Pt/ZrO_2(5)$ catalysts were close to those at 673 K, but all the catalysts were rapidly deactivated, as shown in Fig. 1b, and the H_2 formation activities beyond 70 min fell below those at 673 K.

Table 1
Fundamental properties of catalysts.

Catalyst	Specific surface area (m^2/g)	Amount of Pt sites (μmol/g)	H_2 yield at 10 min[a] (%)
$Pt/ZrO_2(1)$	36	6.2	23.6
$Pt/ZrO_2(3)$	45	9.7	25.7
$Pt/ZrO_2(5)$	50	16.4	28.3

[a] At 673 K.

The initial activity of H_2 formation tends to increase with increasing Pt content. This indicates that the amount of active sites (Table 1) is the main factor controlling the H_2 formation activity.

The yields of gaseous products containing carbon at 673 K over various Pt/ZrO_2 catalysts are shown in Table 2. The yield is defined in terms of the carbon mol% compared to that of the supplied ethanol, and represents carbon recovery as gas:

$$\text{Yield (carbon mol\%)} = \left[\frac{\text{carbon mol of product}}{\text{carbon mol of EtOH feed}}\right] \times 100$$

The main products on the $Pt/ZrO_2(3)$ catalyst were CH_4, CO, and CO_2 in yields of about 32 carbon mol%, 5 carbon mol%, and 35 carbon mol%, respectively, with slight variations depending on the reaction time. Under the conditions used, ethanol conversion was almost 100% in the range 0–220 min. The reaction pathways expected in the ethanol conversion under the conditions adopted are shown in Scheme 1 [7,22,23]. In this study, the yield of CO_2 almost agreed with that of CH_4, and ethanol conversion was almost 100%; it was therefore concluded that CO_2 was formed through the partial steam reforming reaction (i). On the other hand, CO may be formed through ethanol decomposition (ii). If CO_2 is the primary product in the steam reforming reaction of ethanol on some catalysts, and the reverse water gas shift reaction (RWGS) takes place subsequently, as stated by Aupretre et al. [8], CO formation at 673 K should be thermodynamically restricted. The reactive behavior of the catalytic system in this work suggested that reactions (i) and (ii) are competitive, and that the rate of the partial steam reforming reaction (i) is greater than that of the decomposition reaction (ii).

$C_2H_5OH + 3H_2O \rightarrow 2CO_2 + 6H_2$ (0) ($EtOH/H_2O$ complete reforming)
$C_2H_5OH + H_2O \rightarrow CO_2 + 2H_2$ (i) ($EtOH/H_2O$ partial reforming)
$C_2H_5OH \rightarrow CO + 2H_2$ (ii) (EtOH decomposition)
$C_2H_5OH \rightarrow CH_3CHO + 2H_2$ (v) (dehydrogenation)
$C_2H_5OH + C_2H_5OH \rightarrow CH_3COCH_3 + CO + 2H_2$ (vi) (acetone formation)
$C_2H_5OH + H_2O \rightarrow CH_3COOH + H_2$ (vii) (acetic acid formation)
$C_2H_5OH \rightarrow C_2H_4 + H_2O$ (viii) (dehydration)
$CH_4 + H_2O \rightarrow CO + 3H_2$ (iii) (CH_4/H_2O reforming)
$CO + H_2O \rightarrow CO_2 + H_2$ (iv) (WGSR)
$CH_3CHO + H_2O \rightarrow CH_4 + CO_2 + H_2$ (ix) acetaldehyde steam reforming
$CH_3COCH_3 + 2H_2O \rightarrow 3CO + 5H_2$ (x) (acetone steam reformation)

Scheme 1. Reaction pathways expected in ethanol conversion.

From the CO_2 (α, mol/min) and CO (β, mol/min) formation rates, the H_2 (x, mol/min) formation rate from routes (i) and (ii) on the $Pt/ZrO_2(3)$ catalyst is estimated to be *ca.* 1.4 mmol/min, using the equation $x = 2\alpha + \beta$, based on the reaction formulas. This value corresponds to a 25% H_2 yield, and it is almost equal to the observed H_2 yield shown in Fig. 1. This shows that reactions (i) and (ii) are the main H_2 formation routes in this catalytic system. The yield of CH_4 was slightly less than the sum of the CO_2 and CO yields. Considering that only small amounts of acetaldehyde and acetone were detected as liquid products (0.1–0.7 carbon mol% of acetaldehyde, and 0.1–0.4 carbon mol% of acetone for the $Pt/ZrO_2(3)$ catalyst at 673 K), and that the amounts of acetaldehyde and acetone escaping as vapor from the ice trap were very small (<0.5 carbon mol% as yield), this discrepancy suggests that the steam reforming reaction of CH_4 (iii) may proceed to some extent under these conditions.

The overall formation activities of gaseous products containing carbon for the catalysts loaded with large amounts of Pt were high and they were very stable with respect to time-on-stream. Furthermore, it was found that the CO_2/CO ratios in the product gas were also high for the $Pt/ZrO_2(3)$ and $Pt/ZrO_2(5)$ catalysts. On the other hand, the formation rates of gases containing carbon on

Table 2
Yields (C mol%) of CH_4, CO, and CO_2 for steam reforming reaction of reagent ethanol at 673 K.

Catalyst	Product	Time-on-stream (min)						
		10	40	70	100	130	160	190
$Pt/ZrO_2(1)$	CH_4	35.1	31.4	30.7	29.3	27.5	24.7	22.1
	CO	11.5	10.5	10.6	10.7	10.7	10.5	10.2
	CO_2	23.9	21.0	20.1	18.8	16.7	14.0	11.5
$Pt/ZrO_2(3)$	CH_4	32.2	30.4	31.8	32.6	29.2	29.8	31.5
	CO	5.0	4.3	4.5	5.5	3.9	4.6	5.4
	CO_2	35.0	33.8	35.0	34.4	33.2	32.2	33.6
$Pt/ZrO_2(5)$	CH_4	44.5	39.9	37.2	41.3	38.3	38.8	38.8
	CO	10.1	12.0	10.4	11.0	9.8	9.8	8.9
	CO_2	38.1	34.2	31.7	35.8	32.9	33.5	33.3

Table 3
Yields (C mol%) of CH_4, CO, and CO_2 for steam reforming reaction of reagent ethanol at 773 K.

Catalyst	Product	Time-on-stream (min)						
		10	40	70	100	130	160	190
$Pt/ZrO_2(1)$	CH_4	2.4	0.7	0.5	0.4	0.3	0.2	0.2
	CO	2.1	0.4	0.2	0.0	0.0	0.0	0.0
	CO_2	8.8	4.9	5.0	5.0	5.2	4.4	4.0
$Pt/ZrO_2(3)$	CH_4	28.7	3.0	2.1	1.5	1.4	0.9	0.7
	CO	10.8	2.1	1.4	1.0	0.8	0.4	0.3
	CO_2	35.2	11.3	10.7	10.1	10.6	8.4	7.4
$Pt/ZrO_2(5)$	CH_4	42.8	24.0	4.8	3.2	2.0	1.5	1.2
	CO	12.1	11.8	3.7	2.4	1.4	0.9	0.6
	CO_2	45.4	37.1	15.4	15.3	11.2	10.2	9.0

Table 4
Yields (C mol%) of liquid products and ethanol conversion of reagent ethanol at 773 K on $Pt/ZrO_2(3)$.

Product	Time-on-stream (min)						
	25	55	85	115	145	175	205
EtOH conversion	64.8	71.2	63.8	58.2	53.5	56.9	48.9
MeOH	0.0	0.0	0.0	0.0	0.0	0.0	0.0
Acetaldehyde	1.5	1.2	1.2	1.3	1.6	1.6	2.1
Acetone	4.2	4.6	5.4	5.9	5.5	4.4	4.6
Acetic acid	0.0	0.0	0.0	0.0	0.0	0.0	0.0

$Pt/ZrO_2(1)$ decreased with time-on-stream, and the CO_2/CO ratio also greatly decreased. The CO yield (%) is almost constant with time-on-stream. This means that $Pt/ZrO_2(1)$, which has a small amount of Pt sites, tended to undergo strong poisoning at the active sites for the ethanol partial steam reforming reaction. However, since the H_2 yield estimated from the sum of the CO_2 and CO yields almost agrees with the overall H_2 yield observed, it is clear that side reactions (for example (v), (vi), and (vii)), which are accompanied by H_2 formation, were not major reaction routes. In fact, only about 5 carbon mol% of acetaldehyde and 0.5 carbon mol% of acetone were detected in the liquid products, and acetic acid was not detected at all. Under such conditions, the decomposition of ethanol by pathway (ii) is significant.

The yields of CH_4, CO, and CO_2 on the various catalysts at 773 K are shown in Table 3 as a function of the time-on-stream. The formation of gases containing carbon rapidly decreased with time-on-stream, and the degrees of deactivation were larger than those at 673 K. Since no significant sintering of Pt particles was detected in the XRD patterns, regardless of the Pt content, the increased deactivation at 773 K may result from rapid coking rather than from Pt sintering (see Section 3.4).

Although the product distributions after 10 min at 773 K were very similar to those at 673 K, except for the case of $Pt/ZrO_2(1)$, the activity of CH_4 formation decreased rapidly with the time-on-stream, and almost ceased after 100 min. Considering that the thermodynamic equilibrium for the reforming reaction of methane (iii) ($CH_4 + H_2O \rightarrow CO + 3H_2$) is not sufficiently favorable at this temperature, the disappearance of CH_4 formation cannot be explained by promotion of reaction (iii). Ethanol conversion estimated from the effluent liquid at 773 K decreased from 70% to 50% with time-on-stream (see Table 4). Therefore, the deactivation of methanation indicates that the active sites of the partial steam reforming reaction (i) and of the ethanol decomposition reaction (ii) both ceased after 100 min (for $Pt/ZrO_2(1)$ at 10 min) at 773 K. A little CO and CO_2 formation may proceed through routes that do not form CH_4 after the reforming reaction has been deactivated. Given that the amount of carbon deposited at 773 K is much larger than at 673 K (see Section 3.4), it has been suggested that such coking consumes the source of CH_4 as C_1 radicals, and the deposited coke influences the active sites for reactions (i) and (ii).

Vargas et al. [17] reported that the deactivation of CH_4 formation is faster than deactivation of CO_2 and CO formation in ethanol steam reforming, and that ethylene, acetaldehyde, and acetone formation rates are rapidly enhanced, concomitant with the deactivation of H_2 formation, after reacting for 10 h. Table 4 shows the yields of liquid products and ethanol conversion on $Pt/ZrO_2(3)$ at 773 K as a function of time-on-stream. About 6 carbon mol% of acetone (as yield) was formed at 115 min, but the amount is less than the difference between the amounts of (CO_2 + CO) and CH_4 formed. Lack of CH_4 cannot therefore be explained by acetone formation alone, although acetone formation is responsible for a little H_2 formation at higher time-on-stream regions. The yield of acetaldehyde gradually increased, and reached 2 carbon mol% at 220 min. This suggested that acetaldehyde formation is also connected with H_2 formation, but did not directly explain the deactivation of methanation. The analysis of the deactivation mechanism under such conditions will be discussed in Section 3.4.

3.2. Behavior of steam reforming reaction of bio-ethanol

The H_2 yields for the bio-ethanol conversion reaction at 673 K on the various catalysts are shown in Fig. 2a as a function of time-on-stream. The initial activities (at 10 min) were smaller than those for reagent ethanol. Furthermore, even for the catalysts with large Pt loadings, the activities rapidly decreased with time-on-stream; the activities after 190 min were much smaller than those for reagent ethanol. The ratios of the H_2 yields at 190 min to the initial values were 0.29, 0.49, and 0.71 for $Pt/ZrO_2(1)$, $Pt/ZrO_2(3)$, and $Pt/ZrO_2(5)$, respectively. It is clear that the deactivation is more noticeable for catalysts with smaller Pt loadings. This indicates that the observed deactivation of the catalysts was caused by poisoning of the active sites because sintering of Pt metal particles often occurs in support catalysts with large metal loadings. Vargas et al. [17] reported that the H_2 formation rate from bio-ethanol is faster than that from

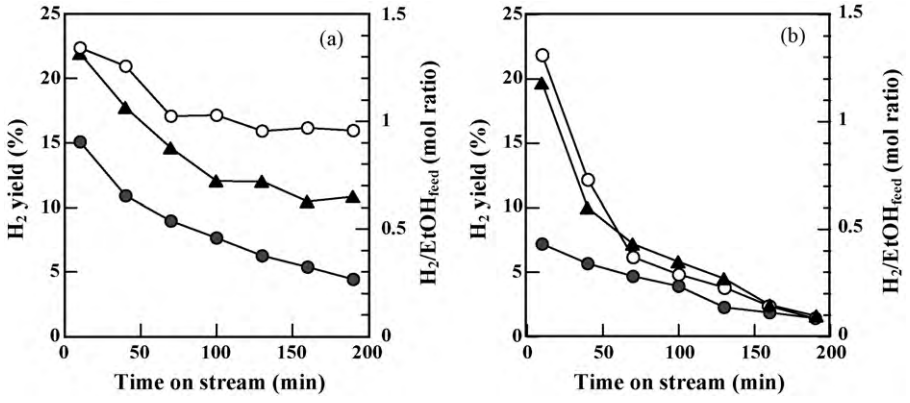

Fig. 2. H_2 yield (%) for bio-ethanol steam reforming reaction at 673 K (a) and at 773 K (b); (●) $Pt/ZrO_2(1)$, (▲) $Pt/ZrO_2(3)$, and (○) $Pt/ZrO_2(5)$. Right ordinate means ratio of H_2 formation rate (mol/min) to EtOH feed rate (mol/min).

Table 5
Yields (C mol%) of CH_4, CO, and CO_2 for steam reforming reaction of the bio-ethanol at 673 K.

Catalyst	Product	Time-on-stream (min)						
		10	40	70	100	130	160	190
	CH_4	33.0	24.1	18.6	16.3	13.4	10.7	8.3
$Pt/ZrO_2(1)$	CO	27.3	26.5	20.6	19.5	16.4	8.1	11.2
	CO_2	11.3	3.0	2.3	1.9	1.7	1.2	0.9
	CH_4	44.6	38.1	34.2	26.5	26.5	26.9	25.6
$Pt/ZrO_2(3)$	CO	15.0	19.0	21.7	18.6	20.5	22.5	19.5
	CO_2	37.5	25.7	17.8	13.2	11.3	8.7	10.9
	CH_4	40.1	38.6	31.5	29.9	30.4	30.6	29.5
$Pt/ZrO_2(5)$	CO	10.7	13.2	11.6	12.6	14.4	15.9	17.2
	CO_2	38.0	33.9	26.2	24.0	21.8	20.9	19.4

the model substance (aqueous ethanol solution) as a result of the existence of other alcohols besides ethanol. On the other hand, Rass-Hansen et al. [18] reported that when using bio-ethanols containing sugars and higher alcohols, catalyst lifetimes ($NiMg/Al_2O_3$, KNi/Mg, Al_2O_3, and $Ru/MgAl_2O_4$) decrease slightly as a consequence of the increased amount of carbon-containing compounds, and of the nature of these compounds. This resulted in a higher rate of carbon formation because of enhancement of the rate by contaminants. However, in our work, severe deactivation, even at short times-on-stream, was observed for bio-ethanol. This suggests that there is another deactivation mechanism in the bio-ethanol reforming reaction in addition to that seen in the reagent ethanol reaction. The severe deactivation may be caused by contaminants other than the carbon-containing compounds.

The yields of CH_4, CO, and CO_2 on the various catalysts at 673 K are shown in Table 5 as a function of the time-on-stream. At 10 min, the formation rates of the gases are as high as those for reagent ethanol, and the product distributions are also similar. However, the overall activity rapidly decreased with time-on-stream; the deactivation of CO_2 formation is particularly remarkable. However, the CO yields on the $Pt/ZrO_2(3)$ and $Pt/ZrO_2(5)$ catalysts slightly increased as opposed to a decrease in the CO_2 yields. Rass-Hansen et al. also reported similar phenomena for the reaction of bio-ethanol containing higher alcohols over $Ru/MgAl_2O_3$ catalyst at 673 K [18], although the catalyst deactivation in their report was slow. In our work, the sum of the CO_2 and CO yields in the catalyst systems is almost equal to the yield of CH_4. It is therefore concluded that the activity in the partial steam reforming reaction of ethanol (i) declined at an early stage, resulting in a relative increase in selection of the ethanol decomposition reaction (ii). Taking into account the rapid deactivation of CO_2 formation for the catalysts with small Pt loadings, this suggested that impurities (other than higher alcohols, as discussed by Rass-Hansen et al.) in the bio-ethanol selectively poison the active sites for the steam reforming reaction, and suppress CO_2 formation. The effects of these materials on catalytic deactivation will be discussed in the next section.

The H_2 yields on the various catalysts at 773 K are shown in Fig. 2b as a function of the time-on-stream. The initial activities were comparable to those at 673 K, but the H_2 yield decreased rapidly by up to 1–2% after 190 min, although the degree of deactivation did not depend strongly on the amount of Pt loading. Although H_2 yields rapidly decreased with time-on-stream even for reagent ethanol (Fig. 1b), it seems that at 773 K bio-ethanol deactivated the catalysts more strongly. The relatively rapid deactivation for bio-ethanol at 773 K indicated that at this higher temperature the impurities in the bio-ethanol may form materials that cannot be removed from the catalyst surface.

The yields of CH_4, CO, and CO_2 on the various catalysts at 773 K are shown in Table 6 as a function of time-on-stream. As with the reactive profile for reagent ethanol, the yields of CO_2 and CH_4 formation rapidly decreased with time-on-stream, showing that the deactivation mechanism for bio-ethanol at 773 K partly resembles that for reagent ethanol. However, the deactivation of CH_4 formation for bio-ethanol was more rapid than that for reagent ethanol. When bio-ethanol was used as the reactant at 773 K, the amount of carbon deposition was larger than that for reagent ethanol (see Section 3.4). These findings suggest that contaminants in the bio-ethanol, or materials derived from them during the reaction, promote coking. CH_4 formation is then more strongly suppressed than it is in the case of reagent ethanol. In addition, maximum acetone formation occurs at a shorter time-on-stream than it does for reagent ethanol. The faster acetone formation for bio-ethanol may also restrict CH_4 formation.

3.3. *Effects of contaminants on catalytic deactivation*

In order to examine the cause of the special deactivation in the bio-ethanol steam reforming reaction, catalytic tests with $Pt/ZrO_2(3)$ were carried out using an aqueous solution of reagent ethanol with added impurities. Fig. 3 shows the time dependence of the H_2 yield in the reaction at 673 K for aqueous ethanol solutions containing 1 wt% acetaldehyde, 0.1 wt% sucrose, or 0.1 wt%

Table 6
Yields (C mol%) of CH_4, CO, and CO_2 for steam reforming reaction of the bio-ethanol at 773 K.

Catalyst	Product	Time-on-stream (min)						
		10	40	70	100	130	160	190
	CH_4	2.1	0.7	0.4	0.3	0.1	0.1	0.1
$Pt/ZrO_2(1)$	CO	2.0	0.5	0.2	0.0	0.0	0.0	0.0
	CO_2	7.5	6.6	5.6	4.8	3.3	3.1	2.7
	CH_4	14.6	3.1	1.7	1.2	0.7	0.4	0.3
$Pt/ZrO_2(3)$	CO	13.1	2.5	1.3	0.7	0.4	0.0	0.0
	CO_2	24.5	10.3	8.1	7.1	5.7	3.2	2.2
	CH_4	39.0	7.7	3.2	2.1	1.2	0.7	0.5
$Pt/ZrO_2(5)$	CO	8.1	5.5	2.5	1.5	0.8	0.3	0.0
	CO_2	44.1	15.6	8.8	6.4	4.4	3.8	2.1

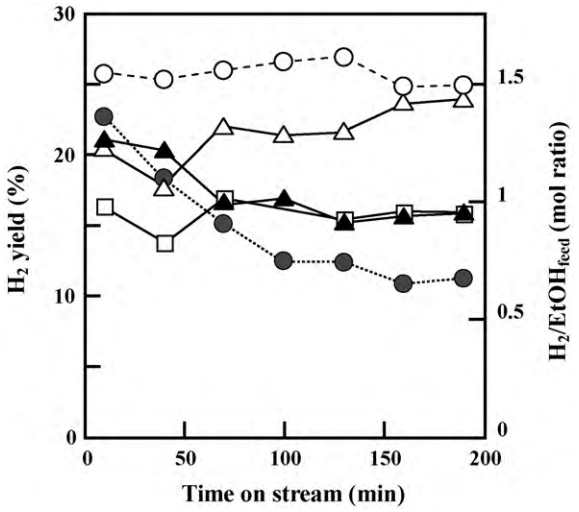

Fig. 3. H_2 yield (%) on $Pt/ZrO_2(3)$ in the steam reforming reaction of ethanol at 673 K for various reactants; (○) regent ethanol, (●) bio-ethanol, (△) ethanol aqueous solution with 1% added acetaldehyde, (□) ethanol aqueous solution with 0.1% added sucrose, and (▲) ethanol aqueous solution with 0.1% added sulfurous acid solution. Right ordinate means ratio of H_2 formation rate (mol/min) to EtOH feed rate (mol/min).

sulfurous acid solution (Wako Pure Chemicals Industry, Ltd., Osaka, Japan; >5 wt% as SO_2). Acetaldehyde is a major impurity in bio-ethanol, and may be formed from ethanol by a side reaction. Here, the concentration of acetaldehyde was adjusted to 1 wt% because the 1.7 wt% of acetaldehyde included in the bio-ethanol was diluted by the water used to bring the H_2O/C_2H_5OH molar ratio to 3. Sugars are known to cause coking in the biomass steam reforming reaction [24]. Although they were not detected in the bio-ethanol used in this study, given the possibility of the existence of trace amounts of sugars such as maltose in bio-ethanol [18,19], as well as the their potential poisoning effects on the reaction, a sample containing 0.1 wt% sucrose was examined. Sucrose was selected as a model impurity. Sucrose is a disaccharide as well as maltose, and glucose and fructose, which are formed by hydrolysis of sucrose, are bio-ethanol source materials. Sulfur is often present in biomass in the form of various chemical species, and it is well known that residual sulfur compounds in a reactant can easily poison the active sites in precious-metal-catalyzed reactions. In addition, the bio-ethanol used in this study was produced through a sulfurous acid treatment of corn. It is important to clarify the poisoning effect of sulfur in bio-ethanol. Although residues of sulfur species in the bio-ethanol could not be detected by the supplier, a sample containing added sulfurous acid was prepared. From the solubility of SO_2 in water, the SO_2 concentration in the model solution was estimated to be 50–100 ppm; this may not be detected by conventional analytical methods. Methanol, which is a major impurity in bio-ethanol, was omitted as a model impurity because it is more easily reformed by water.

For the sample containing acetaldehyde, the activity of H_2 formation and the time dependence of the reaction were very similar to the values for reagent ethanol, showing that acetaldehyde does not significantly affect the activity of H_2 formation. So, we can say that an acetaldehyde content of 1 wt% is not a major factor in deactivation in the bio-ethanol reforming process. On the other hand, the activity of H_2 formation was lowered by the addition of sucrose and sulfurous acid, showing that these materials have poisoning effects for this catalytic system. In particular, it should be noted that the deactivation profile for the sample containing sulfurous acid closely resembled that for the bio-ethanol.

Table 7
Yields of CH_4, CO, and CO_2 for the contaminated solutions[a] at 673 K at 100 min on $Pt/ZrO_2(3)$.

Contaminate	Product yield (C mol%)		
	CH_4	CO	CO_2
Bio-ethanol	26.5	18.6	13.2
Reagent ethanol	32.6	5.5	34.4
Acetaldehyde	35.6	11.2	30.8
Sucrose	23.5	6.4	21.7
Sulfurous acid	27.1	14.1	17.4

[a] Contaminated solutions were containing 1% acetaldehyde, 0.1% sucrose, and 0.1% of sulfurous acid solution (>5% as SO_2), respectively.

The product distributions of CH_4, CO, and CO_2 for the contaminated samples at 673 K at 100 min are compared in Table 7. These contaminants lowered the activity of overall carbonaceous gas formation. The addition of sucrose lowered the activity, but this product distribution does not correspond to that for bio-ethanol; in the bio-ethanol reaction deactivation was accompanied by an increase in CO selectivity and a decrease in CO_2 selectivity. The addition of sulfurous acid to the reactant enhanced the selectivity of CO formation, and the product distribution resembled that for bio-ethanol. These results indicate that the special deactivation in the bio-ethanol reaction in this work may have been brought about by sulfurous acid rather than by acetaldehyde or sugars. Although sucrose was not responsible for the deactivation in the bio-ethanol reaction, it is clear that it is able to poison the Pt/ZrO_2 catalyst. When bio-ethanol contains of the order of 0.1% sugars, attention must paid to catalyst selection and/or purification of the bio-ethanol.

We examined the effects of the contaminants on the reaction at 773 K. Under the reaction conditions, even the catalysts in the reaction with reagent ethanol were rapidly deactivated, but small amounts of the impurities seem to promote more significant deactivation. This indicates that the deactivation at 773 K was mainly caused by coking, as shown in the next section, and the impurities in the bio-ethanol may have promoted this coking.

3.4. Change in catalyst properties by reaction

In order to examine the deactivation mechanism of the catalysts for the bio-ethanol reaction, XPS of the S(2p) core level for the $Pt/ZrO_2(1)$ and $Pt/ZrO_2(3)$ catalysts, before and after reaction for 3 h, was performed (Fig. 4). The reduced $Pt/ZrO_2(1)$ catalysts (after H_2 reduction and before reaction) did not have a peak in the S(2p) region, but an S(2p) peak at around 168 eV appeared in the catalysts after reaction with bio-ethanol for 3 h at 673 K. Since the peak position shifted to the high-energy side, and the surface S content was comparable with the Pt content measured by XPS (S/Pt atom ratios were 0.76, 0.85, and 0.55 for $Pt/ZrO_2(1)$, $Pt/ZrO_2(3)$, and $Pt/ZrO_2(5)$, respectively), the sulfur species would deposit on the catalyst surface as a metal sulfate or metal sulfite. No S(2p) peak appeared in the catalysts after the reaction with reagent ethanol. From these results, we conclude that the rapid catalytic deactivation at 673 K for the bio-ethanol reaction was brought about by the poisoning effects of sulfur species on the Pt sites. Under such conditions, the partial steam reforming reaction (i) may be inhibited, and the decomposition of ethanol (ii) may take place as an alternative reaction.

The S(2p) peak was not detected in the catalysts after reaction at 773 K, even for bio-ethanol. Although the cause is not yet clear, the large amount of carbon deposited on the surface might affect the formation of surface sulfur species at 773 K. The absence of sulfurs suggests that the deactivation at 773 K was not directly caused by sulfur deposition on the Pt sites.

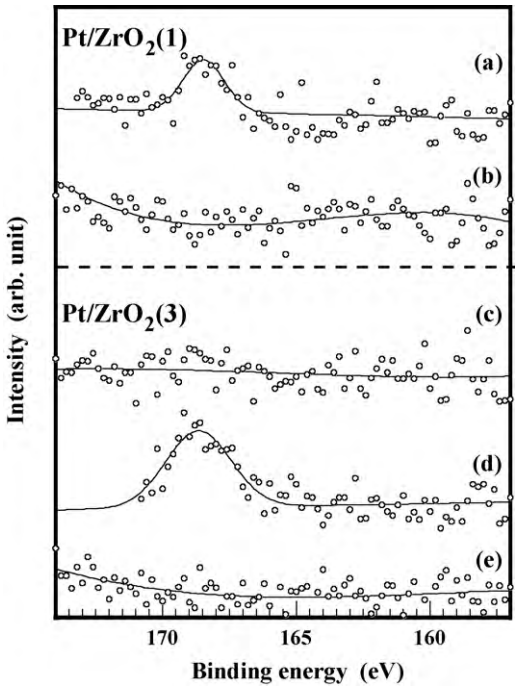

Fig. 4. XPS of S(2p) in catalysts reacted for 3 h: (a) $Pt/ZrO_2(1)$ after reaction with bio-ethanol at 673 K, (b) $Pt/ZrO_2(1)$ before reaction (reduced), (c) $Pt/ZrO_2(3)$ after reaction with bio-ethanol at 773 K, (d) $Pt/ZrO_2(3)$ after reaction with bio-ethanol at 673 K, and (e) $Pt/ZrO_2(3)$ after reaction with reagent ethanol at 673 K.

Fig. 5 shows the C(1s) core-level XPS spectra of the catalysts after the bio-ethanol reaction for 3 h at 673 K and at 773 K. The XPS peak of C(1s) at around 285 eV was enhanced for the catalysts after reaction at 773 K. This peak can be assigned to hydrocarbons and/or graphitic carbons, showing that a large amount of carbon species was deposited on the catalysts after the reaction with bio-ethanol at 773 K. On the other hand, the C(1s) peak intensity after the reaction at 673 K was almost equal to that before reaction. Rass-Hansen et al. reported that the rates of carbon formation on Ni- and Ru-based catalysts were enhanced by decreasing the operating temperature [18]. This discrepancy, as well as the nature of the

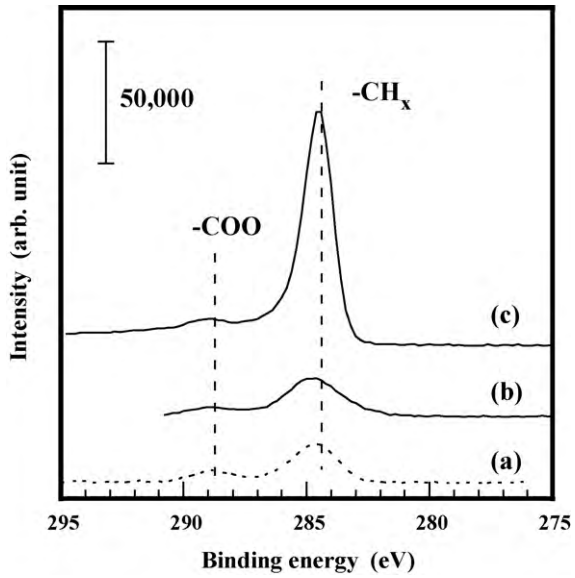

Fig. 5. C(1s) XPS of $Pt/ZrO_2(3)$ after reacting for 3 h with the bio-ethanol: (a) before reaction, (b) after reaction at 673 K, and (c) after reaction at 773 K.

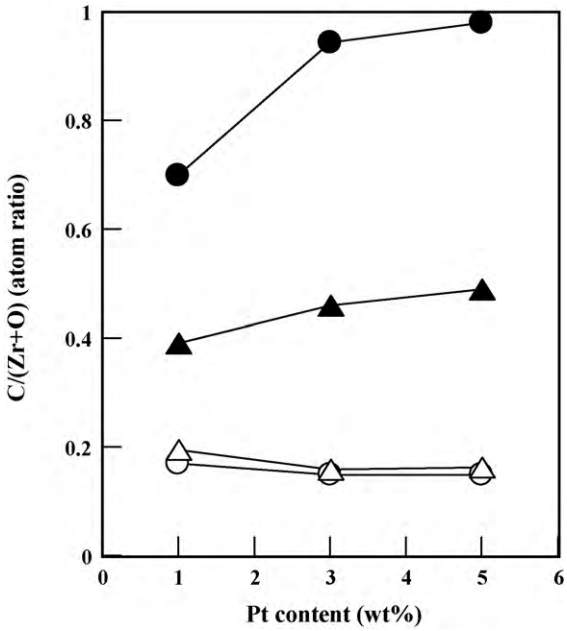

Fig. 6. C/(Zr + O) atomic ratios of the catalysts reacted for 3 h; (△) at 673 K with reagent ethanol, (▲) at 773 K with reagent ethanol, (○) at 673 K with bio-ethanol, and (●) at 773 K with bio-ethanol.

catalyst, may be responsible for the low ratio of carrier gas to reactant gas in our work. Vargas et al. [17] examined Co/Ce/Zr complex oxide catalysts after ethanol steam reforming at 813 K using the temperature-programmed oxidation (TPO) method, and hypothesized that a filament-like carbon deposited on the catalyst surface was responsible for deactivation. Although we could not detect filament carbon on the catalysts in the reaction at 773 K by scanning electron microscopy (SEM), such deposition of carbon species corresponding to the C(1s) peak at 285 eV, which was enhanced after the reaction at high temperature, may be strongly correlated with the deactivation in the reaction with bio-ethanol at 773 K.

In order to investigate the carbon deposits on the surface, the amount of carbon deposited was estimated from the XPS peak intensities of C(1s), Zr(3p), and O(1s). The C/(Zr + O) atomic ratios of the catalysts after reaction for 3 h are shown in Fig. 6. The carbon deposit on the catalysts after reaction at 673 K was small, regardless of the reactants, and the amount of deposit was almost equal to that in the fresh catalyst (before reaction). At 773 K, the carbon deposit increased to twice that for reagent ethanol at 673 K, and up to four times that for the bio-ethanol reaction at 673 K. The C/(Zr + O) atom ratio on the catalyst surface after reaction at 773 K was about 1 for bio-ethanol, indicating that most of the catalyst surface was covered by carbon. The larger amount of carbon deposited for bio-ethanol at 773 K than that deposited for reagent ethanol at 773 K may be caused by an impurity in the bio-ethanol. Rass-Hassen et al. said that the slightly higher rate of carbon formation in the bio-ethanol steam reforming reaction was responsible for carbon-containing compounds in feeds other than ethanol [18]. However, the higher alcohols and sugars discussed as carbon sources in their work are very small in the bio-ethanol reactant used in our work. Therefore, acetaldehyde and/or sulfur species included in the bio-ethanol may have promoted coking on the catalyst surface.

The specific surface areas of the catalysts after reaction for 3 h are shown in Fig. 7. The surface areas decreased after reaction for both reactants, and the decrease is prominent after the reaction at the higher temperature. The crystal structure of the support and its crystal size were unchanged after the reaction, so blocking of the pores in the catalyst by the deposited coke could be respon-

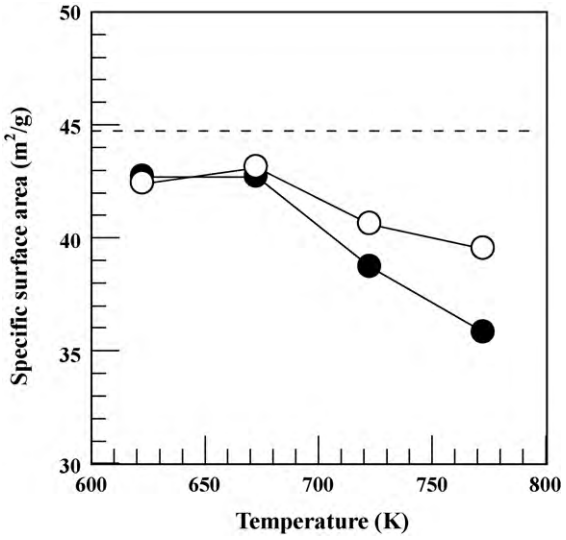

Fig. 7. Specific surface areas of the catalysts reacted for 3 h. (○) Reagent ethanol and (●) bio-ethanol.

sible for the reduction in the surface area; the large amount of carbon deposited at 773 K, as shown in the XPS analysis, blocked some of the nanopores on the zirconia supports. However, the degree of deactivation exceeds the reduction in the surface area, suggesting that the Pt active site was selectively poisoned by carbon. In addition, the larger reduction in surface area after the bio-ethanol reaction at the higher temperature compared with that for the reagent ethanol reaction indicates that the impurities in the bio-ethanol have promoted coking and blocking of the nanopores.

4. Conclusions

The steam reforming reactions for bio-ethanol and reagent ethanol over several Pt/ZrO_2 catalysts with 1–5 wt% Pt loadings were examined. For the reaction with reagent ethanol, the main products were H_2, CO_2, CO, and CH_4; production of acetone, acetaldehyde, and ethylene at 673 K was very low. The partial ethanol steam reforming reaction ($C_2H_5OH + H_2O \rightarrow CO_2 + CH_4 + 2H_2$) and the ethanol decomposition reaction ($C_2H_5OH \rightarrow CH_4 + CO + H_2$) occur competitively in the catalytic system. The activities of the catalysts with larger Pt loadings were higher and more stable. The H_2 yield on the $Pt/ZrO_2(5)$ catalyst reached 29% at 673 K, but at 773 K the activity of H_2 formation rapidly decreased with time-on-stream. The activity for the ethanol steam reforming reaction decreased more rapidly than that for the ethanol decomposition reaction.

The activity of H_2 formation for the reaction with bio-ethanol was lower than that for reagent ethanol, and the CO_2/CO ratio in the product gas was also smaller for bio-ethanol than for reagent ethanol. The deactivation for the bio-ethanol reaction was faster than that for the reagent ethanol reaction, and the deactivation profile with respect to the time-on-stream resembled that for reagent ethanol with 0.1% of added sulfurous acid solution. Furthermore, surface sulfur species were detected on the catalysts reacted with bio-ethanol for 3 h at 673 K. It was therefore concluded that sulfur species in the bio-ethanol poisoned the active Pt sites during the steam reforming process. Although sugars affected the ethanol steam reforming reaction, they were not responsible for the deactivation of the steam reforming reaction for the bio-ethanol used in this work. The deactivation for bio-ethanol at 773 K was more rapid than that for reagent ethanol at 773 K, showing that the large amount of carbon deposited on the catalyst surface was mainly responsible for the deactivation, and that impurities in the bio-ethanol may have promoted coking.

References

[1] M. Sato, A. Kato, Kagaku Sochi 48 (3) (2006) 40.
[2] K. Miwa, Environ. Conserv. Eng. 34 (2005) 171.
[3] Y. Saito, Kagaku Sochi 48 (10) (2006) 42.
[4] JASO Standard, M361-06 (2006).
[5] K. Vasudeva, N. Mitra, P. Umasankar, S.C.X. Dhingra, Int. J. Hydrogen Energy 21 (1996) 13.
[6] H. Song, L. Zhang, R.B. Watson, D. Braden, U.S. Ozkan, Catal. Today 129 (2007) 346.
[7] A. Haryanto, S. Fernando, N. Urali, S. Adhikari, Energy Fuels 19 (2005) 2098.
[8] F. Aupretre, C. Descorme, D. Duprez, Catal. Commun. 3 (6) (2002) 263.
[9] F. Aupretre, C. Descorme, D. Duprez, D. Casanave, D. Uzio, J. Catal. 233 (2005) 464.
[10] J. Comas, F. Mariñ̃o, M. Laborde, N. Amadeo, Chem. Eng. J. 98 (2004) 61.
[11] B. Zhang, X. Tang, Y. Li, W. Cai, Y. Xu, W. Shen, Catal. Commun. 7 (2006) 367.
[12] M.A. Goula, S.K. Kontou, P.E. Tsiakaras, Appl. Catal. B 49 (2004) 135.
[13] A. Simson, E. Waterman, R. Farrauto, M. Castaldi, Appl. Catal. B 89 (2009) 58.
[14] P. Ciambelli, V. Palma, A. Ruggiero, Appl. Catal. B 96 (2010) 190.
[15] J.R. Rostrup-Nielesen, N. Hojlund, in: J. Oudar, H. Wise (Eds.), Deactivation and Poisoning of Catalyst, Marcel Dekker, New York, Basel, 1985, p. 57.
[16] J. Llorca, N. Homs, J. Sales, P. Ramirez de la Piscina, J. Catal. 209 (2002) 306.
[17] J.C. Vargas, S. Libs, A.-C. Roger, A. Kiennemann, Catal. Today 107/108 (2005) 417.
[18] J. Rass-Hansen, R. Johansson, M. Møller, C.H. Christensen, Int. J. Hydrogen Energy 33 (2008) 4547.
[19] A.J. Akande, R.O. Idem, A.K. Dalai, Appl. Catal. A: Gen. 287 (2005) 159.
[20] M. Asadullah, S. Itoh, K. Kunimori, M. Yamada, K. Tomishige, J. Catal. 208 (2002) 255.
[21] K. Takanabe, K. Aika, K. Seshan, L. Lefferts, J. Catal. 227 (2004) 101.
[22] J. Llorca, N. Homs, J. Sales, P. Ramirez de la Piscina, J. Sales, N. Homs, Chem. Commun. (2001) 641.
[23] F. Marino, M. Boveri, G. Baronetti, M. Laborde, Int. J. Hydrogen Energy 26 (2001) 665.
[24] M. Marquevich, S. Czernik, E. Chornet, D. Montane, Energy Fuels 13 (1999) 1160.